^{147}Sm-^{143}Nd systematics of Earth are inconsistent with a superchondritic Sm/Nd ratio

Shichun Huang[1], Stein B. Jacobsen[1], and Sujoy Mukhopadhyay[1]

Department of Earth and Planetary Sciences, Harvard University, Cambridge, MA 02138

Edited by Mark H. Thiemens, University of California at San Diego, La Jolla, CA, and approved February 15, 2013 (received for review December 19, 2012)

The relationship between the compositions of the Earth and chondritic meteorites is at the center of many important debates. A basic assumption in most models for the Earth's composition is that the refractory elements are present in chondritic proportions relative to each other. This assumption is now challenged by recent ^{142}Nd/^{144}Nd ratio studies suggesting that the bulk silicate Earth (BSE) might have an Sm/Nd ratio 6% higher than chondrites (i.e., the BSE is superchondritic). This has led to the proposal that the present-day ^{143}Nd/^{144}Nd ratio of BSE is similar to that of some deep mantle plumes rather than chondrites. Our reexamination of the long-lived ^{147}Sm-^{143}Nd isotope systematics of the depleted mantle and the continental crust shows that the BSE, reconstructed using the depleted mantle and continental crust, has ^{143}Nd/^{144}Nd and Sm/Nd ratios close to chondritic values. The small difference in the ratio of ^{142}Nd/^{144}Nd between ordinary chondrites and the Earth must be due to a process different from mantle-crust differentiation, such as incomplete mixing of distinct nucleosynthetic components in the solar nebula.

chondrite composition | Earth composition | midocean ridge basalt | Sm-Nd isotopic system | nucleosynthetic anomalies

Reliable estimates of the compositions of the bulk silicate Earth (BSE) and depleted mantle (DM), which is the source of midocean ridge basalts (MORBs), are important in determining the degree of mantle processing and the thermal evolution of our planet. Chondritic meteorites have provided the most accurate basis for estimating the compositions of the Sun and planets (1). However, the Earth's chemical composition is overall not chondritic; it has long been known that Earth is depleted in volatile elements (e.g., K) relative to chondrites (2). The assumption that the refractory elements (e.g., rare earth elements) in the Earth are present in chondritic proportions relative to each other is the basis for most estimates of the compositions of the BSE and DM (1, 3–6). This assumption has recently been challenged by several ^{142}Nd/^{144}Nd studies. Specifically, the ^{142}Nd/^{144}Nd of the Earth is ~20 ppm higher than that of the ordinary chondrites (7–9). There are three ways to produce the observed ^{142}Nd difference between the Earth and chondrites (10): (*i*) nucleosynthetic anomalies due to variations of either initial ^{146}Sm/^{144}Sm or initial ^{142}Nd/^{144}Nd ratios in the solar system (11, 12); (*ii*) difference in the Sm/Nd ratio between the BSE and chondrites (8, 13–15); and (*iii*) the BSE has a chondritic Sm/Nd ratio, but an early formed reservoir with a low ^{142}Nd/^{144}Nd ratio is hidden at the base of the mantle (7) or was eroded from the Earth by impacts (16), such that the accessible portion of the BSE has a high ^{142}Nd/^{144}Nd ratio.

Because of the short life (<200 Ma) of the oceanic crust, the extraction of the continental crust (CC) is the only major process depleting the Earth's mantle. Consequently, the DM is complementary to the CC (3, 4). The sum of the CC and DM is the BSE in cases *i* and *ii*, and it is the accessible portion of the BSE in case *iii*, referred to as the "early depleted reservoir" (EDR) by Boyet and Carlson (7). These three scenarios have different implications for the composition of the BSE. In case *i*, the BSE and the chondritic reservoir have essentially the same Sm/Nd ratio (at a ±1% level). In case *ii*, the sum of the CC and DM is the BSE (8, 13–15), and it has a superchondritic Sm/Nd ratio (~6% higher than the chondritic value). In case *iii*, the sum of the CC and DM is the accessible portion of the BSE (7, 16), and it also has a superchondritic Sm/Nd ratio. Such a superchondritic Sm/Nd ratio leads to a present-day ε_{Nd} of ~+7 for CC + DM (7, 8, 13). Here, ε_{Nd} is the deviation of a sample's ^{143}Nd/^{144}Nd ratio from the chondritic value (17) in parts per 10^4.

A BSE with a ε_{Nd} of +7 is critical to the claim that some basalts sample the primitive mantle (PM) (14, 15). Specifically, lavas from some large igneous provinces (LIPs), such as Baffin Island or West Greenland, which cluster around the 4.5-Ga Geochron in a ^{207}Pb/^{204}Pb-^{206}Pb/^{204}Pb plot, have a ε_{Nd} of ~+7. Moreover, Baffin Island picrites with a ε_{Nd} of ~+7 have the highest terrestrial ^{3}He/^{4}He ratio, up to 50-fold the ratio of air (R/Ra) (18). Because high ^{3}He/^{4}He ratios are often taken as evidence for sampling a PM reservoir, it was concluded that these LIP lavas sample pure PM and do not incorporate any other mantle reservoirs (14, 15). In this scenario, PM has a superchondritic present-day ε_{Nd} of ~+7. However, the high ^{3}He/^{4}He ratios of 30- to 50-fold R/Ra associated with a ε_{Nd} of ~+7 could also result from mixing between PM and recycled slabs (19).

Extinct ^{146}Sm-^{142}Nd System

Subsequent to the publication of Boyet and Carlson (7), several studies have revealed a ε^{142}Nd variation of 0.5 ε-units in chondrites, as well as possible correlations of the ε^{142}Nd variation with nucleosynthetic anomalies in ^{135}Ba, ^{144}Sm, and ^{148}Nd (9, 11, 12, 20) (Fig. 1). Specifically, Earth and some enstatite chondrites have a similar ε^{142}Nd, whereas ordinary chondrites have ε^{142}Nd ~0.2 ε-units lower than that of the Earth, and carbonaceous chondrites have the lowest ε^{142}Nd (up to 0.5 ε-units lower than that of the Earth) (figure 1 of ref. 9). In addition to the ^{142}Nd similarity, Earth and enstatite chondrites have the same isotopic compositions of O, Ca, Ti, and Cr, which are elements that show substantial isotopic variation among different chondrite groups (21, 22). Jacobsen and Wasserburg (17) showed that chondrites have a very homogeneous ^{147}Sm/^{144}Nd ratio (0.1932–0.2000), which was later confirmed by Boyet and Carlson (7). This amount of Sm/Nd variation leads to ~0.1 ε-units ε^{142}Nd variation. In addition, ε^{142}Nd is correlated with ε^{144}Sm [a proton-process (p-process) only isotope], ε^{148}Nd [a rapid neutron capture process (r-process) dominated isotope], and ε^{135}Ba in chondrites, and the Earth plots on the chondrite trends, overlapping with enstatite chondrites (Fig. 1). The ε^{142}Nd variation of 0.5 ε-units in chondrites is most likely of a nucleosynthetic origin (11, 12), resulting from small variations in the distribution of different nucleosynthetic components in the solar nebula. To summarize,

Author contributions: S.H., S.B.J., and S.M. designed research, performed research, analyzed data, and wrote the paper.

The authors declare no conflict of interest.

This article is a PNAS Direct Submission.

[1]To whom correspondence may be addressed. E-mail: huang17@fas.harvard.edu, jacobsen@neodymium.harvard.edu, or sujoy@eps.harvard.edu.

This article contains supporting information online at www.pnas.org/lookup/suppl/doi:10.1073/pnas.1222252110/-/DCSupplemental.

there are sub–ε-level nucleosynthetic anomalies in Ba, Nd, and Sm isotopes in chondrites, implying that the chondritic reservoir is not homogeneous at this level. Consequently, it is inappropriate to claim that Earth and the chondritic reservoir have an ~0.2 ε-units ε^{142}Nd difference.

Because there are multiple pathways for producing a ε^{142}Nd variation (10) and the chondritic reservoir is not homogeneous, ε^{142}Nd is not suitable for investigating whether the BSE, or the sum of the CC and DM, has a superchondritic Sm/Nd ratio.

Long-Lived ^{147}Sm-^{143}Nd System

The long-lived ^{147}Sm-^{143}Nd system is not very sensitive to small nucleosynthetic anomalies between chondrites and the Earth because of much larger ^{143}Nd variation due to radioactive decay (many ε units, compared with sub–ε-level variations in ^{142}Nd/^{144}Nd). Therefore, we use the ^{147}Sm-^{143}Nd isotopic system in MORBs and the CC to test whether the BSE could have a superchondritic ^{147}Sm/^{144}Nd ratio with a present-day ε_{Nd} of +7

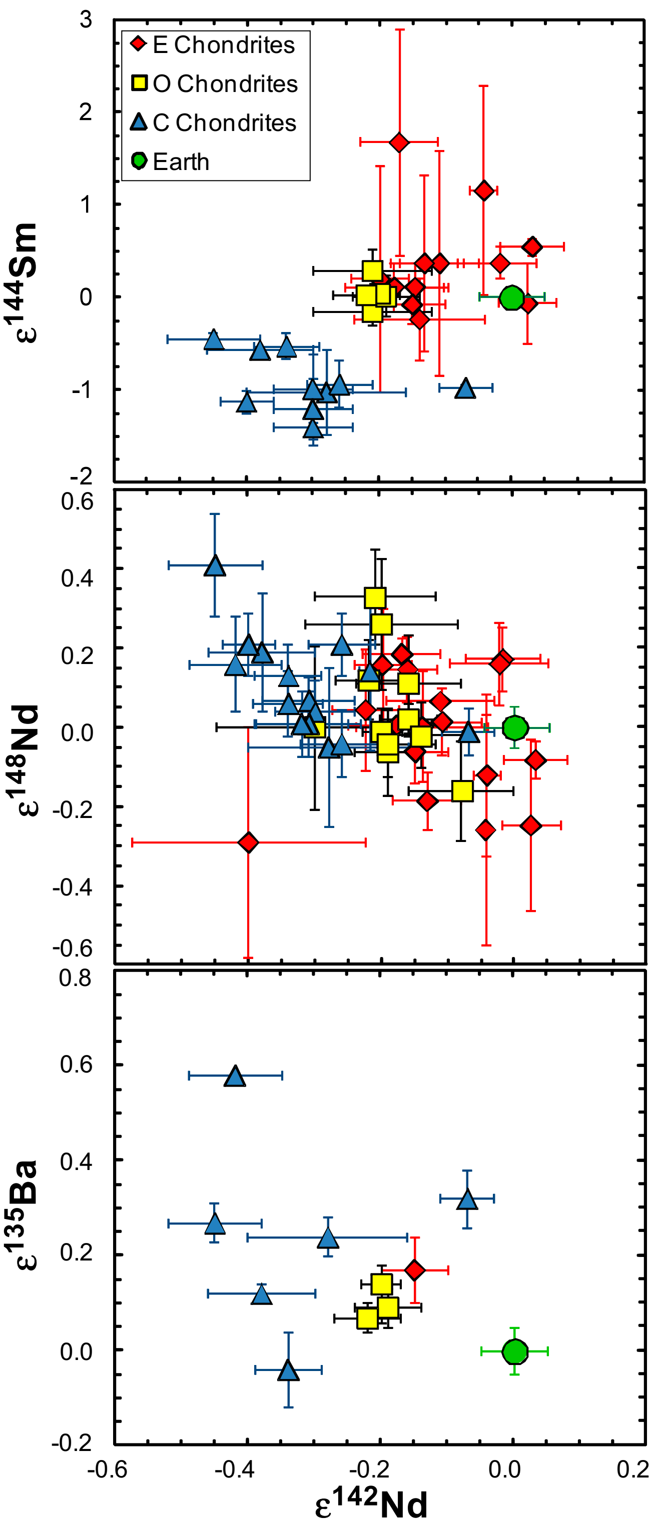

Fig. 1. Variations in ^{144}Sm/^{152}Sm (or ^{144}Sm/^{154}Sm), ^{148}Nd/^{144}Nd, and ^{135}Ba/^{136}Ba vs. ^{142}Nd/^{144}Nd for chondrites. Isotopic ratios are expressed using ε-notation (parts per 10,000) relative to the Earth. ^{144}Sm is a pure p-process isotope, and ^{148}Nd is an r-process dominated isotope. The error bars for the Earth are taken as 5 ppm, which represents the best analytical uncertainty currently available in these isotopic measurements. The Earth plots within the chondrite trends. These trends imply a nucleosynthetic origin for the ^{142}Nd variation in chondrites. The ~0.5 ε-units ε^{142}Nd variation in chondrites does not allow a statement that the Earth and the chondritic reference point have an ~0.2 ε-units difference in ε^{142}Nd (7). Similar plots have also been presented elsewhere (9, 35) showing correlations among these isotopic anomalies. Data are taken from refs. 7, 9, 12, and 20.

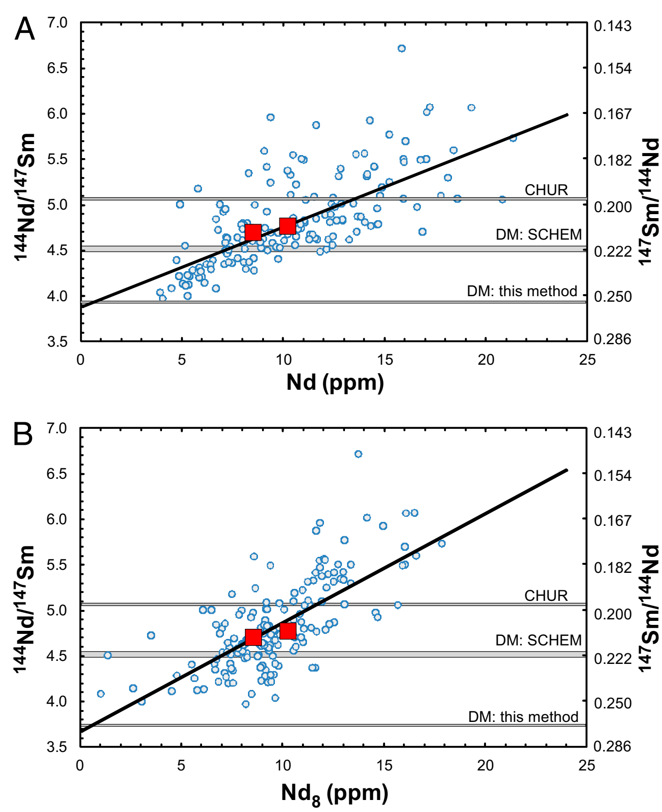

Fig. 2. (*A*) ^{144}Nd/^{147}Sm vs. Nd (parts per million) for MORB samples (blue circles) for which Sm and Nd concentrations have been determined by isotope dilution (sample selection is provided in *SI Text* and Datasets S1 and S2). The average compositions of MORBs from normal ridge segments (red squares) (29, 30) are shown for comparison. The solid line is a robust linear least square regression obtained using MATLAB (MathWorks), and it passes through the estimated average compositions of MORBs from normal ridge segments. It has a slope of 0.088 ± 0.013 (2σ), an intercept of 3.88 ± 0.14 (2σ), and a linear correlation coefficient R^2 of 0.48. The estimated ^{147}Sm/^{144}Nd ratio of the DM is 0.255 ± 0.010 (*SI Text*). Also shown are estimates of the chondritic ^{147}Sm/^{144}Nd ratio (0.1966) (17) and estimates of the ^{147}Sm/^{144}Nd ratio of the DM for the SCHEM (0.217–0.222) (13, 23). (*B*) ^{144}Nd/^{147}Sm vs. Nd_8 (in parts per million by weight) for MORB samples (blue circles) (sample selection is provided in *SI Text* and Datasets S1 and S2). Nd_8 values are Nd concentrations corrected to 8% (wt/wt) MgO following the method of Langmuir et al. (27) (Dataset S2). This trend has a slope of 0.120 ± 0.018 (2σ), an intercept of 3.66 ± 0.18 (2σ), and a linear correlation coefficient R^2 of 0.51. The estimated ^{147}Sm/^{144}Nd ratio of the DM is 0.269 ± 0.013 (*SI Text*).

or higher. That the DM is complementary to the CC is widely used in literature to support both the chondritic Earth model and superchondritic Earth models (SCHEM) (3–6, 13, 23); consequently, the BSE composition can be reconstructed by summing the CC and DM. In a ^{143}Nd/^{144}Nd vs. ^{147}Sm/^{144}Nd plot, the CC, BSE, and DM should all plot on a common isochron, with the CC-BSE and DM-BSE tie-lines having the same slopes. Their slopes give the Sm-Nd model age of the CC in the simple case of a single continent formation event; that is, the age of the CC calculated from the resulting mantle depletion is equivalent to the age of the CC calculated from its ^{147}Sm-^{143}Nd isotopic composition. This single-event age is very close to the mean age of the CC for a more realistic model of forming the CC by a continuous process of melt-extraction over Earth history. If CC recycling is important (24), this single-event Sm-Nd model age could be many hundred million years younger than the average age of the CC (4). Nevertheless, if the ^{147}Sm/^{144}Nd and ^{143}Nd/^{144}Nd ratios of the DM and CC could be determined independently, they would provide a simple test of whether the BSE has a superchondritic ^{147}Sm/^{144}Nd ratio.

The ^{147}Sm/^{144}Nd ratio of the DM has previously been estimated by assuming either a chondritic (5, 6) or a superchondritic (13) BSE composition and a mean age of CC extraction (4, 25) that depleted the mantle (1.5–2.2 Ga). Boyet and Carlson (7, 23) offered a slightly different view of how the DM was generated. They started with a chondritic BSE, but global silicate differentiation within the first 30 Ma generated an EDR (7) with a superchondritic ^{147}Sm/^{144}Nd ratio (ε_{Nd} of ~+7.5) and an early crust [early enriched reservoir (EER)] with a subchondritic ^{147}Sm/^{144}Nd ratio. The EER was hidden at the base of the mantle after its formation and is inaccessible to mantle volcanism. In this scenario, the EDR is the accessible portion of the Earth, from which the CC was extracted to form the DM. A ^{147}Sm/^{144}Nd ratio of 0.229–0.249 for the DM was inferred using a chondritic BSE (5, 6), and a ^{147}Sm/^{144}Nd ratio of 0.217–0.222 for the DM was inferred if the BSE or the accessible portion of the BSE is superchondritic (13, 23).

We note that Boyet and Carlson (7) used a $t_{1/2}$ of 103 Ma for ^{146}Sm, which has been redetermined to be 68 Ma (26). Using this more recently measured $t_{1/2}$, the early silicate differentiation in the model of Boyet and Carlson (7) has to occur within 20 Ma after the formation of the solar system (i.e., before Earth was fully accreted).

Estimating the ^{147}Sm/^{144}Nd Ratio of the DM

Testing whether the Earth has a chondritic or superchondritic ^{147}Sm/^{144}Nd ratio requires the ^{147}Sm/^{144}Nd of the DM to be estimated independent of the BSE composition.

MORBs are partial melts of the DM; thus, we use the Sm and Nd concentrations in MORBs to estimate the average ^{147}Sm/^{144}Nd ratio of the DM. There are three scenarios: (*i*) the DM has a homogeneous ^{147}Sm/^{144}Nd ratio, and the ^{147}Sm/^{144}Nd ratio variations in MORBs are caused by partial melting only; (*ii*) ^{147}Sm/^{144}Nd ratio variations in MORBs only reflect source heterogeneity; and (*iii*) ^{147}Sm/^{144}Nd ratio variations in MORBs reflect both partial melting effects and source heterogeneity. Although Langmuir et al. (27) demonstrated that the majority of the elemental variations in MORBs are controlled by variable degrees of partial melting, we note that the first two scenarios represent two end-member models. Thus, we estimate the average ^{147}Sm/^{144}Nd ratio of the DM for the first two scenarios (*SI Text*).

If the ^{147}Sm/^{144}Nd ratio variations in MORBs are only caused by variable degrees of partial melting (scenario *i*), the ^{147}Sm/^{144}Nd ratio of the DM can be estimated using a method highlighted by Hofmann et al. (28). In this approach, the intercept of the MORB trend in a ^{144}Nd/^{147}Sm vs. Nd diagram is very close to the ^{144}Nd/^{147}Sm ratio of their mantle source. Available Nd and Sm concentrations for MORBs, determined by

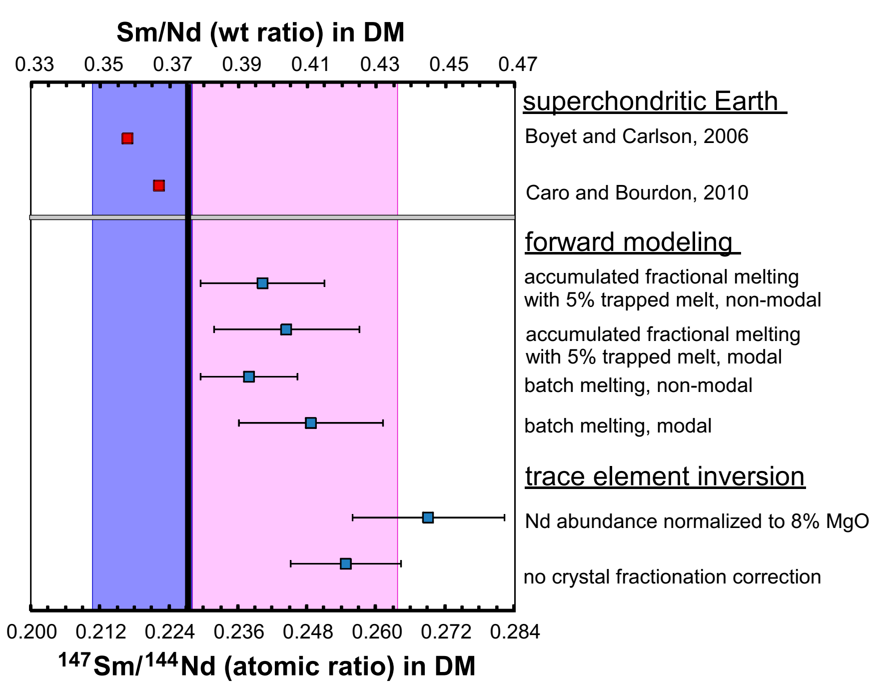

Fig. 3. ^{147}Sm/^{144}Nd ratio of the DM estimated by various approaches. Details are provided in *SI Text*. Estimates from the literature are also included for comparison. The pale blue area, ^{147}Sm/^{144}Nd = 0.211–0.227, represents the possible range for the ^{147}Sm/^{144}Nd ratio of the DM under a SCHEM with a present-day ε_{Nd} of +7 and taking into account the possible ranges for the CC (see Fig. 4 legend). The pink area, ^{147}Sm/^{144}Nd = 0.227–0.264, represents the possible range for the ^{147}Sm/^{144}Nd ratio of the DM under a chondritic Earth model. All our DM estimates are higher than those required by the SCHEM but match those required by a chondritic Earth model. Therefore, the result that the ^{147}Sm/^{144}Nd ratios of the DM inferred from MORB data are higher than those required by the SCHEM is robust and not dependent on model details.

the isotope dilution method (*SI Text* and Datasets S1 and S2), define a positive trend in a ^{144}Nd/^{147}Sm vs. Nd plot (Fig. 2*A*). The ^{147}Sm/^{144}Nd ratio of the DM estimated in this way is 0.255 ± 0.010 (2σ). The Nd concentrations, but not the ^{144}Nd/^{147}Sm ratio, in MORBs may also be affected by crystal fractionation. To correct for this effect, we calculate MORB Nd concentrations at 8% (wt/wt) MgO, called Nd_8, following the method of Langmuir et al. (27). The ^{147}Sm/^{144}Nd ratio of the DM estimated from the ^{144}Nd/^{147}Sm vs. Nd_8 correlation (Fig. 2*B*) is 0.269 ± 0.013 (2σ).

In scenario *ii*, where the ^{147}Sm/^{144}Nd ratio variations in MORBs only reflect source heterogeneity, the ^{147}Sm/^{144}Nd ratio of the DM is estimated using a forward partial melting model. The average ^{147}Sm/^{144}Nd ratio in MORBs from normal ridges (29, 30) is 0.212 ± 0.001 ($2\sigma_m$). Using a partial melting degree of 10%, proper mineral-melt partition coefficients (Table S1), and several types of partial melting models (Tables S2 and S3), the ^{147}Sm/^{144}Nd ratio of the DM is estimated to be 0.238–0.248 (*SI Text*). In this approach, the partial melting degree of 10% used for MORB generation is on the higher end (27). In addition, we only consider a spinel peridotite lithology for MORB generation, and arguments that melting of garnet peridotite or garnet pyroxenite is important in MORB generation have been made (26, 31–33). Because $(Sm/Nd)_{garnet}/(Sm/Nd)_{clinopyroxene} > 1$, including garnet in MORB generation would only increase the estimated ^{147}Sm/^{144}Nd ratio of the MORB source. Consequently, the ^{147}Sm/^{144}Nd ratio of the DM estimated in this way is the minimum value.

Because we discussed the two end-member scenarios (*SI Text*), we argue that the ^{147}Sm/^{144}Nd ratio of the DM is constrained

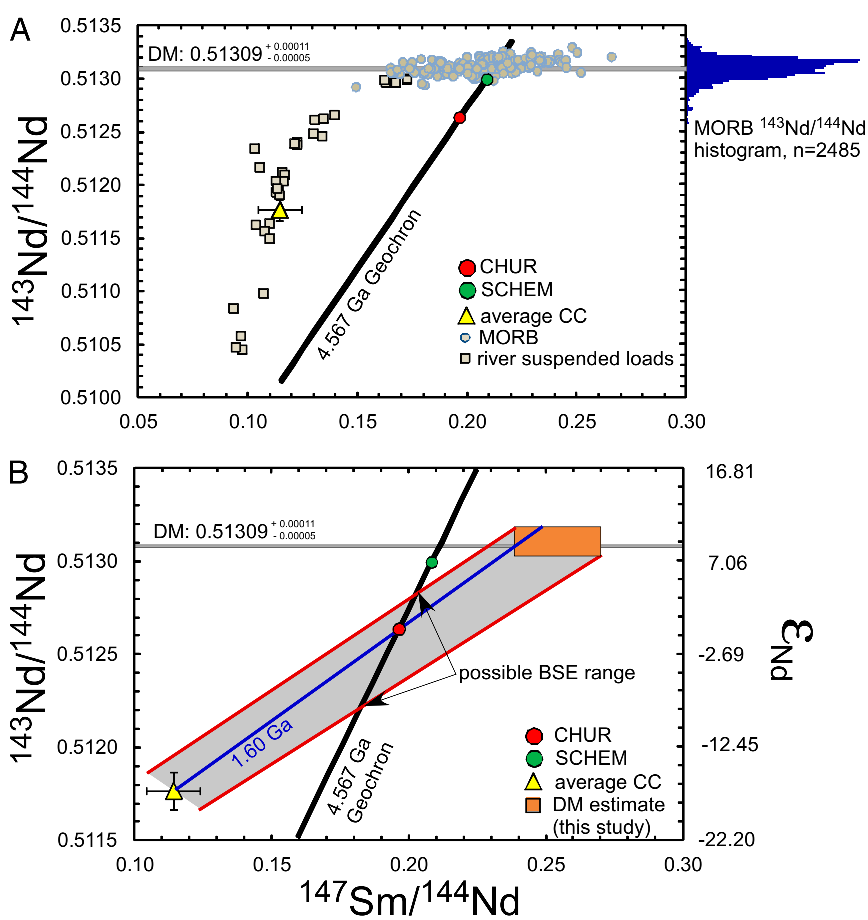

Fig. 4. (*A*) ^{143}Nd/^{144}Nd vs. ^{147}Sm/^{144}Nd isotope systematics of MORBs and river water suspended loads (4, 34). The MORB data in the ^{143}Nd/^{144}Nd vs. ^{147}Sm/^{144}Nd diagram are only MORBs with isotope dilution Sm and Nd measurements ($n = 166$). (*Right*) Histogram of the ^{143}Nd/^{144}Nd ratio for unfiltered MORB samples ($n = 2{,}485$) (*SI Text*) is shown. There is no significant difference between the average ^{143}Nd/^{144}Nd ratio of the two datasets. The ^{143}Nd/^{144}Nd ratios of MORBs show limited variation and form a near-normal distribution with a peak at 0.51318, corresponding to a ε_{Nd} of 10.6. The ε_{Nd} is the ^{143}Nd/^{144}Nd deviation from the chondritic value (CHUR) in parts per 10^4 $\left[\varepsilon_{Nd} = \left(\frac{^{143}Nd/^{144}Nd}{0.512638} - 1\right)10^4\right]$ (17). The ^{143}Nd/^{144}Nd ratio of the DM is inferred to be $0.51309^{+0.00011}_{-0.00005}$, corresponding to a ε_{Nd} of $8.8^{+2.2}_{-1.0}$, and it agrees well with the previously published average ^{143}Nd/^{144}Nd ratio of 0.51311–0.51313 for normal (N)-MORBs (5, 29). For comparison, we also show positions for the chondritic reference values in this diagram (CHUR) (17), a SCHEM (13), an average CC (34) (^{147}Sm/^{144}Nd = 0.114 ± 0.010, ^{143}Nd/^{144}Nd = 0.51177 ± 0.00010), and a 4.567-Ga Geochron. (*B*) ^{143}Nd/^{144}Nd vs. ^{147}Sm/^{144}Nd systematics of major reservoirs in the Earth. The CHUR, SCHEM, and average CC are the same as in *A*. Our estimate of the DM in this diagram (brown box) comes from the ^{147}Sm/^{144}Nd ratio obtained based on MORB data and the Nd isotopic composition from *A* (^{147}Sm/^{144}Nd = 0.238–0.269, ^{143}Nd/^{144}Nd = 0.51304–0.51320). The possible range of the DM-CC tie-line is shown as a gray field outlined by two red lines (by taking the end-member values of DM and CC), and its intersection with the 4.567-Ga Geochron represents our estimated BSE composition (^{147}Sm/^{144}Nd = 0.183–0.204, ^{143}Nd/^{144}Nd = 0.51223–0.51286, and $\varepsilon_{Nd} = -8.0$ to $+4.4$). The CC-CHUR tie-line has a ^{147}Sm-^{143}Nd model age of 1.60 Ga, consistent with the average age of the CC (a detailed discussion is provided in ref. 4). Possible mantle-crust differentiation ages can be estimated by connecting the extreme values of the DM and CC (e.g., the lower right corner of the CC with the upper left corner of the DM). This leads to a mantle-crust differentiation age of 1.1–2.0 Ga, consistent with the age of the CC (4). The CHUR point lies within the possible range of intersections between the CC-DM isochron and the Geochron. The SCHEM point lies substantially above this range. Thus, there is no evidence for a SCHEM based on ^{147}Sm-^{143}Nd isotopic variations in the CC and MORBs.

between 0.238 and 0.269 (Fig. 3). The pale blue area in Fig. 3, where the $^{147}Sm/^{144}Nd$ = 0.211–0.227, represents the possible DM $^{147}Sm/^{144}Nd$ ratio range constrained by the CC composition under a SCHEM with a present-day ε_{Nd} of +7. The pink area, where the $^{147}Sm/^{144}Nd$ = 0.227–0.264, represents the possible DM $^{147}Sm/^{144}Nd$ ratio range constrained by the CC under a chondritic Earth model. All our estimated $^{147}Sm/^{144}Nd$ ratios of the DM are higher than that required for a superchondritic Earth, and agree with those required for a chondritic Earth (Fig. 3). Therefore, the result that the $^{147}Sm/^{144}Nd$ ratio of the DM inferred from MORB data is higher than that required by the SCHEM is robust and not dependent on model details.

Test for a Superchondritic $^{147}Sm/^{144}Nd$ Ratio in the BSE

In a $^{143}Nd/^{144}Nd$ vs. $^{147}Sm/^{144}Nd$ plot, MORBs form a nearly horizontal trend, whereas the river water suspended loads (34), which sample large areas of the CC, form a nearly vertical trend with samples from young arc terrains plotting within the MORB field (Fig. 4*A*). The average $^{147}Sm/^{144}Nd$ and $^{143}Nd/^{144}Nd$ ratios of the CC are well constrained using Sm-Nd isotopic data from river water suspended loads (34) (Fig. 4*A*). The MORB $^{143}Nd/^{144}Nd$ data show limited variation, with a near-normal distribution. Our inferred plausible range of DM $^{143}Nd/^{144}Nd$ ($0.51309^{+0.00011}_{-0.00005}$) covers the central 68% of the MORB histogram (Fig. 4*A*) and is typical of the MORB $^{143}Nd/^{144}Nd$ variations (29).

We now test whether the Earth could have a superchondritic $^{147}Sm/^{144}Nd$ ratio using the $^{147}Sm/^{144}Nd$ and $^{143}Nd/^{144}Nd$ ratios of the DM and CC (Fig. 4*B*). The BSE must be at the intersection of the 4.567-Ga Geochron and the DM-CC tie-line in this diagram. Taking into account the possible DM and CC ranges, the DM-CC tie-line crosses the 4.567-Ga Geochron at a $^{147}Sm/^{144}Nd$ ratio of 0.183–0.204 and a $^{143}Nd/^{144}Nd$ ratio of 0.51223–0.51286 (ε_{Nd} = −8.0 to +4.4). The large uncertainties associated with the intersection of the DM-CC tie-line and the 4.567-Ga Geochron result from the large uncertainties in the $^{147}Sm/^{144}Nd$ and $^{143}Nd/^{144}Nd$ ratios of the DM and CC. This intersection overlaps with the chondritic point; however, even taking into account the large uncertainty, the SCHEM plots well above this intersection (Fig. 4*B*). Moreover, the CC-chondritic uniform reservoir (CHUR) tie-line passes through the possible DM range. This CC-CHUR tie-line has a ^{147}Sm-^{143}Nd model age of 1.60 Ga, consistent with the average age of the CC (a detailed discussion is provided in ref. 4). Therefore, the ^{147}Sm-^{143}Nd isotope systematics of the DM and CC, considered together, are inconsistent with a superchondritic Earth with a present-day ε_{Nd} of +7. Our results demonstrate that the BSE has a near-chondritic $^{147}Sm/^{144}Nd$ ratio.

The existence of a hidden reservoir at the base of the mantle proposed to explain the observed $\varepsilon^{142}Nd$ difference between the Earth and ordinary chondrites (7) is also inconsistent with the ^{147}Sm-^{143}Nd isotope systematics of the CC-DM system, because it requires an extremely young age for the CC. In this case, the accessible portion of the Earth (EDR), from which the CC was extracted, has a present-day ε_{Nd} of +8 to +12 ($^{143}Nd/^{144}Nd$ = 0.51305–0.51325) (7), overlapping with present-day MORB values. Consequently, an EDR-DM tie-line has a near-zero slope, implying an unrealistically young age (approximately zero age) for the CC. Furthermore, because the EDR and DM have the same ε_{Nd}, there is no way to balance the low ε_{Nd} values in the CC. Because loss of an early crust through collisional erosion during the end stages of terrestrial accretion (16) in essence represents a reservoir hidden in space, such a scenario is also inconsistent with the ^{147}Sm-^{143}Nd isotope systematics and can be ruled out.

Assuming a simple CC growth model in which the CC started to grow at 4.4 Ga at a constant rate, Caro and Bourdon (13) have argued that a chondritic Earth model cannot explain the radiogenic ε_{Nd} in the Archean mantle. They argued instead that the positive ε_{Nd} found in the Archean mantle requires a superchondritic bulk Earth $^{147}Sm/^{144}Nd$ ratio (figure 11 of ref. 13). However, using a more realistic CC growth model in which recycling of the CC is allowed, Jacobsen (4) was able to reproduce the trend of radiogenic ε_{Nd} in the Archean mantle with a $^{147}Sm/^{144}Nd$ ratio evolution that is consistent with the updated DM estimate provided in this paper. The evolution curves in Fig. 5 were evaluated by Jacobsen (4) to be consistent with the data available in 1988. For comparison, we show the ε_{Nd} estimates for the average DM compiled in 2010 by Caro and Bourdon (13) and used in their modeling. We also show that the end point of the $^{147}Sm/^{144}Nd$ ratio evolution from Jacobsen (4) is consistent with the estimate given in this paper. Thus, we conclude that the Sm-Nd isotopic evolution of the mantle through time is consistent with a chondritic Earth and that the conclusion of Caro and Bourdon (13) is only valid for a particularly simplistic model calculation.

Conclusions

In summary, the ^{147}Sm-^{143}Nd isotope systematics of the CC and DM imply that the BSE has a near-chondritic $^{147}Sm/^{144}Nd$ ratio and are inconsistent with the BSE having a present-day ε_{Nd} of +7 as required by the SCHEM (7, 8, 13–15). The ~0.5 ε-units $\varepsilon^{142}Nd$ variation in the Earth and chondrites most likely results from variations in the mixing proportions of different nucleosynthetic components. Given the ~0.5 ε-units $\varepsilon^{142}Nd$ variation (7–9, 20) in bulk chondrites but $\leq\pm2\%$ variations in $^{147}Sm/^{144}Nd$ ratios (17), it seems inappropriate to attribute the ~0.2 ε-units $\varepsilon^{142}Nd$ difference between the Earth and ordinary chondrites to a 6% difference in $^{147}Sm/^{144}Nd$ ratios.

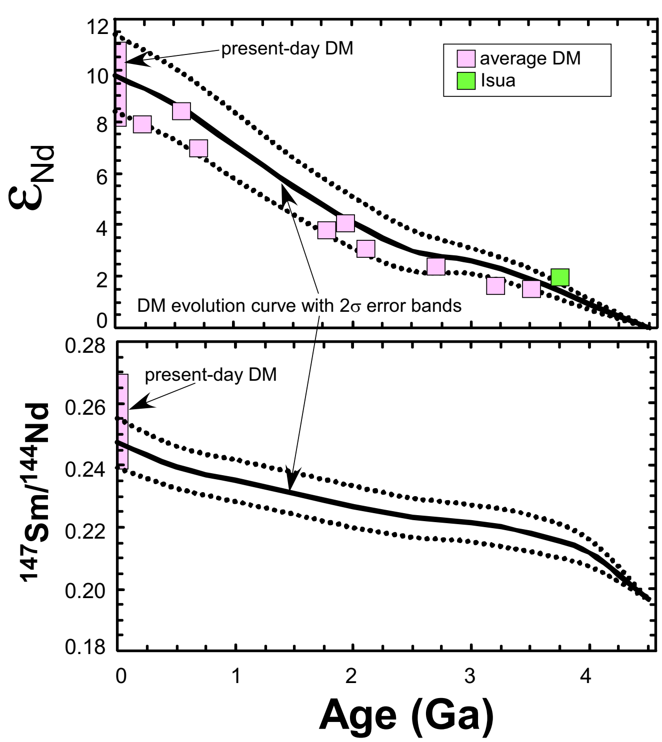

Fig. 5. Model evolution of the DM ε_{Nd} and $^{147}Sm/^{144}Nd$ ratio through time. The data points are average DM compositions and Isua supracrustals from the recent compilation of Caro and Bourdon (13). The present-day DM estimates are from this study. The model curves are from Jacobsen (4) using a chondritic Earth model. The evolution of the DM ε_{Nd} is consistent with a chondritic Earth model with CC recycling (4) but not with a simple CC growth model without CC recycling as presented by Caro and Bourdon (13). Our estimate of the present-day DM $^{147}Sm/^{144}Nd$ ratio is also consistent with the model prediction of Jacobsen (4).

ACKNOWLEDGMENTS. We appreciate discussions on the topic of this paper with A. Brandon, R. W. Carlson, C. Chauvel, T. Elliott, M. Humayun, W. F. McDonough, C. H. Langmuir, R. J. O'Connell, G. J. Wasserburg, and Q. Yin. This work was partly supported by National Science Foundation Awards EAR-1144727 and OCE-0929193 and by National Aeronautics and Space Administration Award NNX12AH65G.

1. McDonough WF, Sun SS (1995) The composition of the Earth. *Chem Geol* 120: 223–253.
2. Wasserburg GJ, Macdonald GJF, Hoyle F, Fowler WA (1964) Relative Contributions of Uranium, Thorium, and Potassium to Heat Production in the Earth. *Science* 143(3605): 465–467.
3. Hofmann AW (1988) Chemical differentiation of the Earth: The relationship between mantle, continental crust and oceanic crust. *Earth Planet Sci Lett* 90:297–314.
4. Jacobsen SB (1988) Isotopic and chemical constraints on mantle-crust evolution. *Geochim Cosmochim Acta* 52:1341–1350.
5. Salters VJM, Stracke A (2004) Composition of the depleted mantle. *Geochemistry Geophysics Geosystems* 5(5):Q05004.
6. Workman RK, Hart SR (2005) Major and trace element composition of the depleted MORB mantle (DMM). *Earth Planet Sci Lett* 231:53–72.
7. Boyet M, Carlson RW (2005) ^{142}Nd evidence for early (>4.53 Ga) global differentiation of the silicate Earth. *Science* 309(5734):576–581.
8. Caro G, Bourdon B, Halliday AN, Quitté G (2008) Super-chondritic Sm/Nd ratios in Mars, the Earth and the Moon. *Nature* 452(7185):336–339.
9. Gannoun A, Boyet M, Rizo H, El Goresy A (2011) 146Sm-142Nd systematics measured in enstatite chondrites reveals a heterogeneous distribution of 142Nd in the solar nebula. *Proc Natl Acad Sci USA* 108(19):7693–7697.
10. Jacobsen SB, et al. (2008) Isotopes as clues to the origin and earliest differentiation history of the Earth. *Philos Transact A Math Phys Eng Sci* 366(1883):4129–4162.
11. Ranen MC, Jacobsen SB (2006) Barium isotopes in chondritic meteorites: Implications for planetary reservoir models. *Science* 314(5800):809–812.
12. Andreasen R, Sharma M (2006) Solar nebula heterogeneity in p-process samarium and neodymium isotopes. *Science* 314(5800):806–809.
13. Caro G, Bourdon B (2010) Non-chondritic Sm/Nd ratio in the terrestrial planets: Consequences for the geochemical evolution of the mantle-crust system. *Geochim Cosmochim Acta* 74:3333–3349.
14. Jackson MG, et al. (2010) Evidence for the survival of the oldest terrestrial mantle reservoir. *Nature* 466(7308):853–856.
15. Jackson MG, Carlson RW (2011) An ancient recipe for flood-basalt genesis. *Nature* 476(7360):316–319.
16. Campbell IH, O'Neill HS (2012) Evidence against a chondritic Earth. *Nature* 483(7391): 553–558.
17. Jacobsen SB, Wasserburg GJ (1984) Sm-Nd isotopic evolution of chondrites and achondrites, II. *Earth Planet Sci Lett* 67:137–150.
18. Stuart FM, Lass-Evans S, Fitton RM, Ellam RM (2003) High ^{3}He/^{4}He ratios in picritic basalts from Baffin Island and the role of a mixed reservoir in mantle plumes. *Earth Planet Sci Lett* 104:364–380.
19. Gonnermann HM, Mukhopadhyay S (2009) Preserving noble gases in a convecting mantle. *Nature* 459(7246):560–563.
20. Carlson RW, Boyet M, Horan M (2007) Chondrite barium, neodymium, and samarium isotopic heterogeneity and early Earth differentiation. *Science* 316(5828):1175–1178.
21. Trinquier A, et al. (2009) Origin of nucleosynthetic isotope heterogeneity in the solar protoplanetary disk. *Science* 324(5925):374–376.
22. Zhang J, Dauphas N, Davis AM, Leya I, Fedkin A (2012) The proto-Earth as a significant source of lunar material. *Nat Geosci* 5:251–255.
23. Boyet M, Carlson RW (2006) A new geochemical model for the Earth's mantle inferred from ^{146}Sm-^{142}Nd systematics. *Earth Planet Sci Lett* 250:254–268.
24. Jackson MG, et al. (2007) The return of subducted continental crust in Samoan lavas. *Nature* 448(7154):684–687.
25. Jacobsen SB, Wasserburg GJ (1979) The mean age of mantle and crustal reservoirs. *J Geophys Res* 84:7411–7427.
26. Kinoshita N, et al. (2012) A shorter 146Sm half-life measured and implications for 146Sm-142Nd chronology in the solar system. *Science* 335(6076):1614–1617.
27. Langmuir C, Klein E, Plank T (1992) Petrological systematics of mid-ocean ridge basalts: Constraints on melt generation beneath ocean ridges. *Mantle Flow and Melt Generation at Mid-Ocean Ridges*, eds Morgan JP, Blackman DK, Sinton JM (American Geophysical Union, Washington, DC), pp 183–280.
28. Hofmann AW, Feigenson MD, Raczek I (1984) Case studies on the origin of basalt: III. Petrogenesis of the Mauna Ulu eruption, Kilauea, 1969-1971. *Contrib Mineral Petrol* 88:24–35.
29. Su YJ (2002) Mid-ocean ridge basalt trace element systematics: Constraints from database management, ICP-MS analyses, global data compilation, and petrologic modeling. PhD thesis (Columbia University, New York).
30. Arevalo R, Jr., McDonough WF (2010) Chemical variations and regional diversity observed in MORB. *Chem Geol* 271:70–85.
31. Hirschmann M, Stolper EM (1996) A possible role for garnet pyroxenite in the origin of the "garnet signature" in MORB. *Contrib Mineral Petrol* 124:185–208.
32. Sobolev AV, et al. (2007) The amount of recycled crust in sources of mantle-derived melts. *Science* 316(5823):412–417.
33. Salters VJM, Hart SR (1989) The hafnium paradox and the role of garnet in the source of mid-ocean-ridge basalts. *Nature* 342(6248):420–422.
34. Goldstein SJ, Jacobsen SB (1988) Nd and Sr isotopic systematics of river water suspended material: Implications for crustal evolution. *Earth Planet Sci Lett* 87:249–265.
35. Qin L, Carlson RW, Alexander CM (2011) Correlated nucleosynthetic isotopic variability in Cr, Sr, Ba, Sm, Nd and Hf in Murchison and QUE 97008. *Geochim Cosmochim Acta* 75:7806–7828.

Supporting Information

Huang et al. 10.1073/pnas.1222252110

SI Text

Midocean Ridge Basalt $^{147}Sm/^{144}Nd$ and $^{143}Nd/^{144}Nd$ Ratio Data

We used the online midocean ridge basalt (MORB) database PetDB (www.petdb.org) (*i*) to find all MORB samples with $^{143}Nd/^{144}Nd$ isotope measurements and (*ii*) to find all samples that have been measured for Nd, Sm, and MgO concentrations in addition to $^{143}Nd/^{144}Nd$ isotope measurements.

We found 2,485 MORB samples, basalts from spreading centers only, with $^{143}Nd/^{144}Nd$ measurements. They form a near-normal distribution with a peak at 0.51318 (Fig. 4*A*), very similar to other estimates of the typical value for the $^{143}Nd/^{144}Nd$ ratio in the MORB source (1, 2). Because the arguments presented in this paper discuss percentage level differences between various estimates of the Sm/Nd ratio of the depleted mantle (DM), it is required that the MORB Sm/Nd data used in this argument have similar or better precision. Thus, only samples with isotope dilution Sm and Nd concentration data were selected because these are typically accurate to at least 1% and are often much better. Furthermore, the samples were screened to include only spreading center basalts with MgO > 6 wt %. This resulted in 166 qualified MORB samples. All these data were checked for correctness with their original data sources. These data are given in the form of an Excel (Microsoft Corporation) spreadsheet (Datasets S1 and S2).

$^{147}Sm/^{144}Nd$ Ratio in the DM: Constraints from MORBs

The elemental variations of MORBs reflect (*i*) variable degrees of partial melting, (*ii*) source heterogeneity, and (*iii*) a combination of these two factors. We consider the first two scenarios, which are the two end-members. In the case that the elemental variations of MORBs reflect only varying degrees of partial melting, we follow an approach first highlighted by Hofmann et al. (3). Considering a batch-melting process, the concentrations of Sm (C_{Sm}) and Nd (C_{Nd}) are given by:

$$\frac{C^l_{Sm}}{C^o_{Sm}}=\frac{1}{D_{Sm}+F(1-D_{Sm})}\ldots\ldots \quad \textbf{[S1]}$$

$$\frac{C^l_{Nd}}{C^o_{Nd}}=\frac{1}{D_{Nd}+F(1-D_{Nd})}\ldots\ldots \quad \textbf{[S2]}$$

where the superscripted *l* represents the melt value and the superscripted *o* represents the source value; *F* is the degree of melting, and D_{Sm} and D_{Nd} are the bulk partition coefficients of Sm and Nd, respectively. By eliminating *F* from Eqs. **S1** and **S2** and replacing the weight ratio with the atomic ratio using $^{147}Sm/^{144}Nd = 0.60492\frac{C^o_{Sm}}{C^o_{Nd}}$, it can be shown that in a plot of $^{144}Nd/^{147}Sm$ vs. C_{Nd} (Fig. 2), the intercept (*I*) gives $\frac{1-D_{Sm}}{1-D_{Nd}}\frac{1}{(^{147}Sm/^{144}Nd)_{source}}$ and the slope (*S*) is $\frac{1-\frac{1-D_{Sm}}{1-D_{Nd}}}{0.60492C^o_{Sm}}$. The following relationship can be obtained from a plot of $^{144}Nd/^{147}Sm$ vs. C_{Nd}:

$$(^{147}Sm/^{144}Nd)_{source}=\frac{1-0.60492SC^o_{Sm}}{I}\ldots\ldots \quad \textbf{[S3]}$$

$$\frac{1-D_{Sm}}{1-D_{Nd}}=1-0.60492SC^o_{Sm}\ldots\ldots \quad \textbf{[S4]}$$

MORB samples, with Sm and Nd concentrations determined by isotope dilution (Datasets S1 and S2), form a positive $^{144}Nd/^{147}Sm$ vs. Nd trend (Fig. 2*A*). A robust linear least square regression using MATLAB (MathWorks) gives a slope (*S*) of 0.088 ± 0.013 and an intercept (*I*) of 3.88 ± 0.14 (both 2σ). Following Eq. **S3**, the Sm concentration in the DM (C^{DM}_{Sm}) is required to calculate the DM $^{144}Nd/^{147}Sm$ ratio. C^{DM}_{Sm} has been estimated as 0.2–0.3 ppm using a chondritic or superchondritic bulk silicate Earth (1, 4, 5). We assign a large uncertainty to C^{DM}_{Sm} (0.2 ± 0.1 ppm). Because *S* is a very small number, $(1-0.60492SC^{DM}_{Sm})$ is not very sensitive to C^{DM}_{Sm}. Using these values, the $^{147}Sm/^{144}Nd$ ratio of the DM is estimated as 0.255 ± 0.010 (2σ).

Using Eq. **S4**, $\frac{1-D_{Sm}}{1-D_{Nd}}$ is estimated as 0.989 ± 0.006, and it can also be independently estimated using previously determined values for D_{Sm} and D_{Nd}. Specifically, D_{Sm} = 0.045 and D_{Nd} = 0.031 are given by Workman and Hart (4) and yield a $\frac{1-D_{Sm}}{1-D_{Nd}}$ of 0.986, matching our estimate based only on MORB data. Salters and Stracke (1) used D_{Sm} = 0.060 and D_{Nd} = 0.020, which give a $\frac{1-D_{Sm}}{1-D_{Nd}}$ of 0.959. This value is slightly lower than our estimate. Using this $\frac{1-D_{Sm}}{1-D_{Nd}}$ value, the estimated $^{147}Sm/^{144}Nd$ ratio of the DM is 0.247 ± 0.010. This value agrees within error with our estimate of 0.255 ± 0.010.

The D_{Sm} and D_{Nd} values can be further constrained using experimental data (Table S1). During MORB generation, the Sm-Nd fractionation is mostly controlled by clinopyroxene, because the partition coefficients of Sm and Nd for orthopyroxene and olivine are a factor of 10–100 lower than that for clinopyroxene (6, 7). Table S1 summarizes available ${D_{Sm}}^{CPX/melt}$ and ${D_{Nd}}^{CPX/melt}$ determined by experiments that are applicable to partial melting at the midocean ridge. ${D_{Sm}}^{CPX/melt}$ ranges from 0.201 to 0.494 with an average of 0.32 ± 0.06 ($2\sigma_m$), and ${D_{Nd}}^{CPX/melt}$ ranges from 0.112 to 0.277 with an average of 0.19 ± 0.03 ($2\sigma_m$), which yield a ${K_{dSm\text{-}Nd}}^{CPX/melt} = {D_{Sm}}^{CPX/melt}/{D_{Nd}}^{CPX/melt}$ of 1.64 ± 0.08 ($2\sigma_m$) (Table S1). If the DM has 20% clinopyroxene, the $\frac{1-D_{Sm}}{1-D_{Nd}}$ is estimated as 0.973 ± 0.017. The uncertainty is estimated using Monte Carlo simulation. We randomly picked 2,000 values for ${D_{Nd}}^{CPX/melt}$ and ${K_{dSm\text{-}Nd}}^{CPX/melt}$, assuming that both ${D_{Nd}}^{CPX/melt}$ (0.19 ± 0.03) and ${K_{dSm\text{-}Nd}}^{CPX/melt}$ (1.64 ± 0.08) define normal distributions. ${D_{Sm}}^{CPX/melt}$ was calculated using ${D_{Nd}}^{CPX/melt}$ and ${K_{dSm\text{-}Nd}}^{CPX/melt}$. This estimate agrees well with our estimate of 0.989 ± 0.006 based on MORB data.

This approach ignores the crystal fractionation effect on MORBs, which affects Nd concentrations but not the $^{147}Sm/^{144}Nd$ ratio. To remove this crystal fractionation effect, we calculate the Nd concentrations at 8% (wt/wt) MgO, Nd_8 (Datasets S1 and S2), following Langmuir et al. (8), and then repeat the above exercise. The $^{144}Nd/^{147}Sm$ vs. Nd_8 trend (Fig. 2*B*) has a slope of 0.120 ± 0.018 (2σ), an intercept of 3.66 ± 0.18 (2σ), and an R^2 of 0.51. Normalization to 8% MgO improves the correlation. The $^{147}Sm/^{144}Nd$ ratio of the DM is then estimated as 0.269 ± 0.013 (2σ). $\frac{1-D_{Sm}}{1-D_{Nd}}$ is estimated as 0.986 ± 0.008 (2σ), agreeing well with experimental partition coefficients (see discussion above).

MORBs form a slightly positive $^{143}Nd/^{144}Nd$ vs. $^{147}Sm/^{144}Nd$ trend (Fig. 4*A*), with an R^2 of 0.26. It is possible that the $^{144}Nd/^{147}Sm$-Nd trend in Fig. 2 partially reflects a mixing line. In the case that the MORB elemental variations reflect only source heterogeneity, we use a forward partial melting model to estimate the DM $^{147}Sm/^{144}Nd$ ratio. Using the data compilation from Arevalo and McDonough (9), the average $^{147}Sm/^{144}Nd$ ratio of *N*-MORB [$(La/Sm)_N < 1$] is 0.212 ± 0.001 ($2\sigma_m$), which is close to previous estimates (0.210–0.211) (2, 9). We use ${D_{Sm}}^{CPX/melt}$ and ${D_{Nd}}^{CPX/melt}$ determined by experiments (Table S1) to estimate the Sm-Nd fractionation during MORB generation. We assume that the DM has 20% clinopyroxene and the average partial melting degree is 10%. Using $D_{Sm}^{CPX/melt}$ and $D_{Nd}^{CPX/melt}$ as summarized in Table S1, we estimate the Sm-Nd fractionation during the partial melting process that generates MORBs (Tables S2 and S3). In detail, $(Sm/Nd)_{DM}/(Sm/Nd)_{N\text{-MORB}}$ ranges from 1.12 to 1.17 according to different partial melting models (Table S2). The DM $^{147}Sm/^{144}Nd$ ratio is estimated to range from 0.238 ± 0.009–0.248 ± 0.013 (Table S3). These uncertainties mainly reflect the uncertainties on $D_{Sm}^{CPX/melt}$ and $D_{Nd}^{CPX/melt}$, and they are estimated using Monte Carlo simulation. Within error, these estimates agree with our estimate based on the $^{144}Nd/^{147}Sm$ vs. Nd correlation (Fig. 3). These values (0.238 ± 0.009–0.248 ± 0.013) are also significantly higher than the $(^{147}Sm/^{144}Nd)_{DM}$ of 0.217–0.222 required by a superchondritic Earth model (SCHEM) (Fig. 3). A 10% degree of partial melting for MORB generation is used in this approach, which is on the high end (8), such that the estimated $^{147}Sm/^{144}Nd$ ratios of DM using this approach (Tables S2 and S3) are minimum estimates.

In the second approach, many Sm and Nd concentrations were not determined by the isotope dilution technique (9). Although it is expected that the large amount of Sm and Nd data used in estimating the average Sm/Nd ratio in *N*-MORBs (2, 9) may provide good statistics if analytical errors are truly random, such an expectation needs to be tested with a large amount of high-precision data.

Each of the DM $^{147}Sm/^{144}Nd$ ratio estimates is model-dependent (degree of partial melting vs. source heterogeneity); however, both DM estimates are higher than those required by the SCHEM (Fig. 3). Therefore, our conclusion that the DM $^{147}Sm/^{144}Nd$ ratios inferred from MORB data are higher than those required by the SCHEM is robust and not dependent on model details.

1. Salters VJM, Stracke A (2004) Composition of the depleted mantle. *Geochemistry Geophysics Geosystems* 5(5):Q05004.
2. Su YJ (2002) Mid-ocean ridge basalt trace element systematics: Constraints from database management, ICP-MS analyses, global data compilation, and petrologic modeling. PhD thesis (Columbia University, New York).
3. Hofmann AW, Feigenson MD, Raczek I (1984) Case studies on the origin of basalt: III. Petrogenesis of the Mauna Ulu eruption, Kilauea, 1969-1971. *Contrib Mineral Petrol* 88:24–35.
4. Workman RK, Hart SR (2005) Major and trace element composition of the depleted MORB mantle (DMM). *Earth Planet Sci Lett* 231:53–72.
5. Boyet M, Carlson RW (2006) A new geochemical model for the Earth's mantle inferred from ^{146}Sm-^{142}Nd systematics. *Earth Planet Sci Lett* 250:254–268.
6. Salters VJM, Longhi J (1999) Trace element partitioning during the initial stages of melting beneath mid-ocean ridges. *Earth Planet Sci Lett* 166:15–30.
7. Eggins SM, Rudnick RL, McDonough WF (1998) The composition of peridotites and their minerals: A laser-ablation ICP-MS study. *Earth Planet Sci Lett* 154:53–71.
8. Langmuir C, Klein E, Plank T (1992) Petrological systematics of mid-ocean ridge basalts: Constraints on melt generation beneath ocean ridges. *Mantle Flow and Melt Generation at Mid-Ocean Ridges*, eds Morgan JP, Blackman DK, Sinton JM (American Geophysical Union, Washington, DC), pp 183–280.
9. Arevalo R, Jr., McDonough WF (2010) Chemical variations and regional diversity observed in MORB. *Chem Geol* 271:70–85.

Table S1. Experimentally determined partition coefficients

	$D_{Sm}^{CPX/melt}$	$D_{Nd}^{CPX/melt}$	$K_{dSm\text{-}Nd}^{CPX/melt}$	Ref(s).
	0.291	0.1873	1.55	1
	0.462	0.277	1.67	2
	0.281	0.177	1.59	3
	0.201	0.112	1.79	4
	0.421	0.260	1.62	4
	0.232	0.141	1.65	4
	0.804	0.494	1.63	4*
	0.359	0.255	1.41	4
	0.211	0.129	1.64	5
	0.293	0.178	1.65	6
	0.253	0.167	1.51	7†
	0.319	0.186	1.72	7†
	0.494	0.258	1.91	7†
Average	0.32	0.19	1.64	
$2\sigma_m$	0.06	0.03	0.08	

*The melt of this experiment is a high-Al melt, and it does not apply to MORB generation. It is excluded in calculating the average.

†Only low-pressure (<2 GPa) experiments are included. These are expected to be appropriate for partial melting of spinel peridotites. Details are provided in a study by Salters and Longhi (7).

1. Hart SR, Dunn T (1993) Experimental CPX/melt partitioning of 24 trace elements. *Contrib Mineral Petrol* 113:1–8.
2. Hauri EH, Wagner TP, Grove TL (1994) Experimental and natural partitioning of Th, U, Pb and other trace elements between garnet, clinopyroxene and basaltic melts. *Chem Geol* 117:149–166.
3. Johnson KTM (1994) Experimental CPX/ and garnet/melt partitioning of REE and other trace elements at high pressures; Petrogenetic implications. *Mineral Mag* 58:454–455.
4. Skulski T, Minarik W, Watson EB (1994) High-pressure experimental trace-element partitioning between clinopyroxene and basaltic melts. *Chem Geol* 117:127–147.
5. Sobolev AV, Migdisov AA, Portnyagin MV (1996) Incompatible element partitioning between clinopyroxene and basalt liquid revealed by the study of melt inclusions in minerals from Troodos lavas, Cyprus. *Petrology* 4:307–317.
6. Johnson KTM (1998) Experimental determination of partition coefficients for rare earth and high-field-strength elements between clinopyroxene, garnet, and basaltic melt at high pressures. *Contrib Mineral Petrol* 133:60–68.
7. Salters VJM, Longhi J (1999) Trace element partitioning during the initial stages of melting beneath mid-ocean ridges. *Earth Planet Sci Lett* 166:15–30.

Table S2. $(Sm/Nd)_{source}/(Sm/Nd)_{melt}$ **according to various melting models**

	Modal melting	Nonmodal melting*
Batch melting, no trapped melt†	1.17 ± 0.06	1.12 ± 0.04
Accumulated fractional melting,† 5% trapped melt	1.15 ± 0.06	1.13 ± 0.05

*Melting reaction from 1.5-Gpa experiment of Kinzler (1): 0.80 CPX + 0.19 OL + 0.13 SP = 0.12 OPX + 1.00 melt, where CPX is clinopyroxene, OL is olivine, OPX is orthopyroxene, and SP is spinel.
†Following Shaw (2).

1. Kinzler RJ (1997) Melting of mantle peridotite at pressure approaching the spinel to garnet transition: Application to mid-ocean ridge basalt petrogenesis. *J Geophys Res* 102:853–874.
2. Shaw DM (1970) Trace element fractionation during anatexis. *Geochim Cosmochim Acta* 34:237–243.

Table S3. $(^{147}Sm/^{144}Nd)_{DM}$ **according to various melting models**

	Modal melting	Nonmodal melting
Batch melting, no trapped melt	0.248 ± 0.013	0.238 ± 0.009
Accumulated fractional melting, 5% trapped melt	0.244 ± 0.013	0.240 ± 0.011

Other Supporting Information Files

Dataset S1 (XLSX)
Dataset S2 (XLSX)